

MHD CONVECTION IN A LID-DRIVEN CAVITY HEATED LINEARLY AT BOTTOM

Subhrajyoti Sarkar^{a,1}, Akash Jha^a, Ritesh Samanta^a, Nirmalendu Biswas^{b,2}
and Nirmal K. Manna^a

^aDepartment of Mechanical Engineering, Jadavpur University, Kolkata 700032, India

^bDepartment of Power Engineering, Jadavpur University, Salt Lake, Kolkata-700106, India

Corresponding author email: ¹subhramath100@gmail.com, ²nirmalendubiswas@yahoo.co.in

Paper received on: March 24, 2020, accepted after revision on: May 14, 2020
10.21843/reas/2019/17-27/196163

ABSTRACT: The impact of magnetic-field induced force on buoyant flow in lid-driven cavity is addressed in this work. Two sides of the cavity are moving in opposite directions. The temperature of heating element located on the bottom wall is varied linearly and is mirrored about the mid-point of the wall. The convective heat transfer in the cavity is analyzed systematically using an in-house CFD code. The fundamental aspects of different flow regimes, the strength and inclination of magnetic field are explored. The obtained results reveal strong influence of Ri and Ha on the heat transfer characterization.

Keywords. MHD convection, Lid-driven cavity, Heat transfer.

NOMENCLATURE

B	magnetic field (Wb/m^2)	x, y	Cartesian coordinates (m)
g	acceleration due to gravity (ms^{-2})	X, Y	dimensionless coordinates
H	cavity height, length scale (m)		
L	cavity length (m)		
			Greek symbols
Ha	Hartmann number	α	thermal diffusivity (m^2s^{-1})
Nu	average Nusselt number	β	expansion coefficient of fluid (K^{-1})
p	pressure (Pa)	θ	dimensionless temperature
P	dimensionless pressure	ν	kinematic viscosity (m^2s^{-1})
Pr	Prandtl number	ρ	density (kgm^{-3})
Re	Reynolds number	ψ	dimensionless streamfunction
Ri	Richardson number	κ	electrical conductivity, $\mu\text{S/cm}$
T	temperature (K)	γ	magnetic field inclination
u, v	velocity components (ms^{-1})		Subscripts
U, V	dimensionless velocity components	a	ambient
U_o	wall/ lid velocity, m/s	c, h	cold/hot wall

1. INTRODUCTION

The magneto-hydrodynamics (MHD) involving buoyant flow in thermal cavities finds many applications in the field of engineering and science. It is an interdisciplinary field. The study of MHD coupled heat transfer can be classified into two major

categories. In the first case the medium is highly conductive and the heat is produced by electromagnetic field. While in the second case the medium is poor conductor, so in compared to the imposed field, the evolved induced field can be neglected.

Heat transfer using natural convection plays a key role in many engineering applications. It can be found in heat exchanger, desiccation technology, electronic technology, solar energy, and greasing technology [1-4]. Sivaraj et al. [5] analyzed MHD natural convection along with entropy generation using ferrofluid and heated plate located centrally in a square cavity. They have found that increasing Hartmann number diminishes the strength of the convective flow and thereby heat transfer, whereas the entropy generation was found to increase irrespective of magnetic-field inclination. Akinsete [6] investigated the effect of aspect ratios a triangular cavity during natural convection. Several investigations were carried out in cavities with obstruction of various shapes [7-8] undergoing natural convection. Saravanan et al. [9] examined natural convection in square cavity with a discrete heater placed inside, in consideration with thermal radiation. Here, with higher Rayleigh number and surface emissivity, the heat transfer is found to increase. Hakan and Derbentli [10] numerically examined convection of air in rectangular cavities. Oztop et al. [11] presented natural convection with volumetric heat generation.

Several earlier investigations have dealt with the influence of magnetic fields on the electrically conducting fluids. The magnetic force has strong influence on convection in thermal devices. Sathiyamoorthy and Chamkha [12] demonstrated the impact of inclined magnetic field on heat transfer in enclosures. Oreper and Szekely [13]

observed weakening of natural convection applying magnetic field. The strength of magnetic field affects the crystal quality of crystal growth process. Ozoe and Maruo [14] studied numerically the magnetic-field melted silicon considering natural convection. Nadezhda et al. [15] numerically analyzed melting process in a square cavity considering MHD natural convection and local heater. The magnetic force affects turbulent solidification process [16]. The present and futuristic developments with lots of examples are reviewed in Kabeel et al. [17].

On the background of the above-mentioned literatures (and many other not reported here for brevity), the present problem is formulated using classical lid-driven cavity and linearly varying heating in triangular form at bottom. The aim of the present study is to analyze the effect of magnetic field on fluid flow and heat transfer under different regimes of convective flow. The investigation is conducted from the fundamental point of view using Richardson number (Ri), Reynolds number (Re), and Hartmann number (Ha) and its inclination angle (γ°). The analysis is reported using isotherms, streamlines and average Nusselt number (Nu).

2. DESCRIPTION OF PROBLEM

In the schematic diagram shown in Fig.1, the working fluid containing in the cavity is electrical conductor and uniform magnetic field (B) is applied externally at an angle(γ°). It has adiabatic sidewalls moving at uniform speed U_0 in vertical direction in opposite

manner. The top wall which acts as a heat sink with ambient temperature (T_c), is used for cooling. The heating element is located along the bottom wall. The heating temperature (T_c) is varying linearly from both the ends (T_c) with maximum temperature (T_h) at the middle. In order to reduce some computational burden, two-dimensional analysis is carried out here.

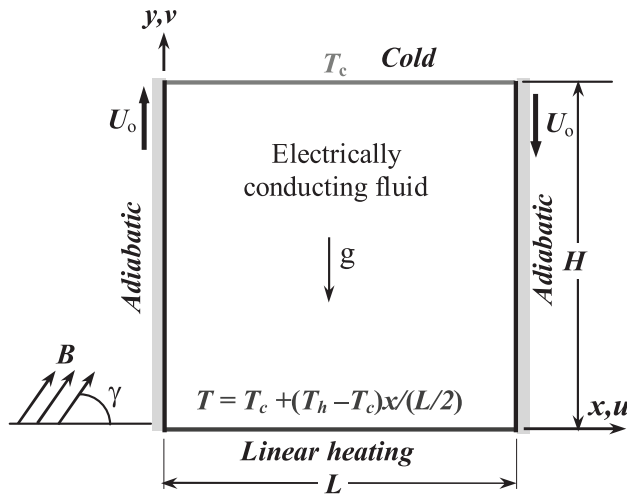


Fig.1. Description of the problem along with boundary conditions

2.1 Formulation and Numerical Techniques

The problem is analyzed considering two-dimensional, Newtonian, incompressible and laminar flow. The magnetic force and buoyancy are taken into account. However, the induced magnetism or Hall effect along with Joule heating is neglected. The buoyancy is modelled using the Boussinesq approximation. Negligible viscous dissipation is ignored. The evolved dimensionless governing equations (in Cartesian coordinate system) are:

$$\frac{\partial U}{\partial X} + \frac{\partial V}{\partial Y} = 0 \quad (1)$$

$$U \frac{\partial U}{\partial X} + V \frac{\partial U}{\partial Y} = -\frac{\partial P}{\partial X} + \frac{1}{\text{Re}} \left(\frac{\partial^2 U}{\partial X^2} + \frac{\partial^2 U}{\partial Y^2} \right) + \frac{Ha^2}{\text{Re}} (U \sin \gamma \cos \gamma - V \sin^2 \gamma) \quad (2)$$

$$U \frac{\partial V}{\partial X} + V \frac{\partial V}{\partial Y} = -\frac{\partial P}{\partial Y} + \frac{1}{\text{Re}} \left(\frac{\partial^2 V}{\partial X^2} + \frac{\partial^2 V}{\partial Y^2} \right) + \frac{Ha^2}{\text{Re}} (V \sin \gamma \cos \gamma - U \cos^2 \gamma) + \text{Ri} \theta \quad (3)$$

$$U \frac{\partial \theta}{\partial X} + V \frac{\partial \theta}{\partial Y} = \frac{1}{\text{Re Pr}} \left(\frac{\partial^2 \theta}{\partial X^2} + \frac{\partial^2 \theta}{\partial Y^2} \right) \quad (4)$$

here, (X, Y) and (U, V) are respectively dimensionless coordinates and components of velocity. P and θ are dimensionless pressure and temperature. The details of these variables are furnished below.

$$(X, Y) = (x, y) / H; \quad (U, V) = (u, v) / U_0;$$

$$P = \frac{(p - p_a)}{\rho U_0^2}; \quad \theta = \frac{(T - T_c)}{(T_h - T_c)} \quad (5)$$

The dimensionless involved parameters are Re , Ri , Pr and Ha , and defined by

$$\text{Re} = \frac{U_0 H}{\nu}; \quad \text{Ri} = \frac{(g \beta (T_h - T_c) H^3 / \nu^2)}{(U_0 H / \nu)^2}; \quad \text{Pr} = \frac{\nu}{\alpha}; \quad \text{Ha} = BH \sqrt{\kappa / \rho \nu} \quad (6)$$

Based on the problem configuration, the wall conditions (Fig. 1) for all variables are given by

- a) $U=0, V=U_o, \frac{\partial \theta}{\partial X} = 0$ for the left adiabatic wall
- b) $U=0, V=-U_o, \frac{\partial \theta}{\partial X} = 0$ for the right adiabatic wall
- c) $U=0, V=0, \theta = 0$ for the top cold wall
- d) $U=0, V=0, \theta = 2X$ for the bottom heating wall

The above-mentioned boundary conditions and the governing equations are solved by an well-validated in-house CFD code [18–20].

The processing and analysis of the results are carried out using heat transfer rate and temperature distribution (isotherms) and flow pattern (streamlines) in the cavity. Under steady condition, the rejection through the top wall is equal to net heat from through the bottom wall. The heat transfer rate is computed using the average Nusselt number (Nu) of top wall, given by

$$Nu = \int_0^1 \left(-\frac{\partial \theta}{\partial Y} \Big|_{Y=1} \right) dX \quad (7)$$

Under steady state, Nu of the bottom and top walls is same. The streamfunction (ψ) is an arbitrary function whose derivatives give velocity components of a particular flow situation. By the definition the lines of constant streamfunction are known as streamlines. As the flow is confined in the cavity, the streamfunction value at the walls is taken as $\psi = 0$.

3. RESULTS AND DISCUSSION

The chosen problem is simulated using $Pr=0.71$, $Ri=0.1-50$, $Re=10-200$, $Ha=0-100$

and $\gamma = 0-180^\circ$. The ranges of these pertinent parameters are selected following earlier works in this area [1, 2, 5, 11, 12]. The flow patterns of heat and fluid are analyzed using streamlines and isotherms. The maximum streamfunction value corresponds to the strength of vortex. The isotherms represent the temperature distribution in the cavity, and the temperature gradients at the heating and cooling walls presents the local heat transfer rate through the walls. The rate of heat transfers from the cavity is realized through the Nusselt number. The results are presented systematically in different sub-section below.

3.1 Effect of Richardson number (Ri)

The plots of streamlines and isotherms for visualizing the flow pattern and temperature distribution are shown in Fig. 2. Three regions of convective heat transfer are captured using $Ri = 0.1$ (forced convection), $Ri = 1$ (mixed convection) and $Ri = 10-50$ ($Ri > 1$, natural convection). As there is no much change in contour plots of $Ri = 0.1$ and $Ri = 1$, the results corresponding to $Ri = 0.1$ is not included in Fig. 2. The figure shows results for $Ri = 1$ (that corresponds to mixed convection) and $Ri = 10, 100$ (correspond to dominating natural convection with different strengths). The streamlines and isotherms are presented successively in the first and second rows of the figure.

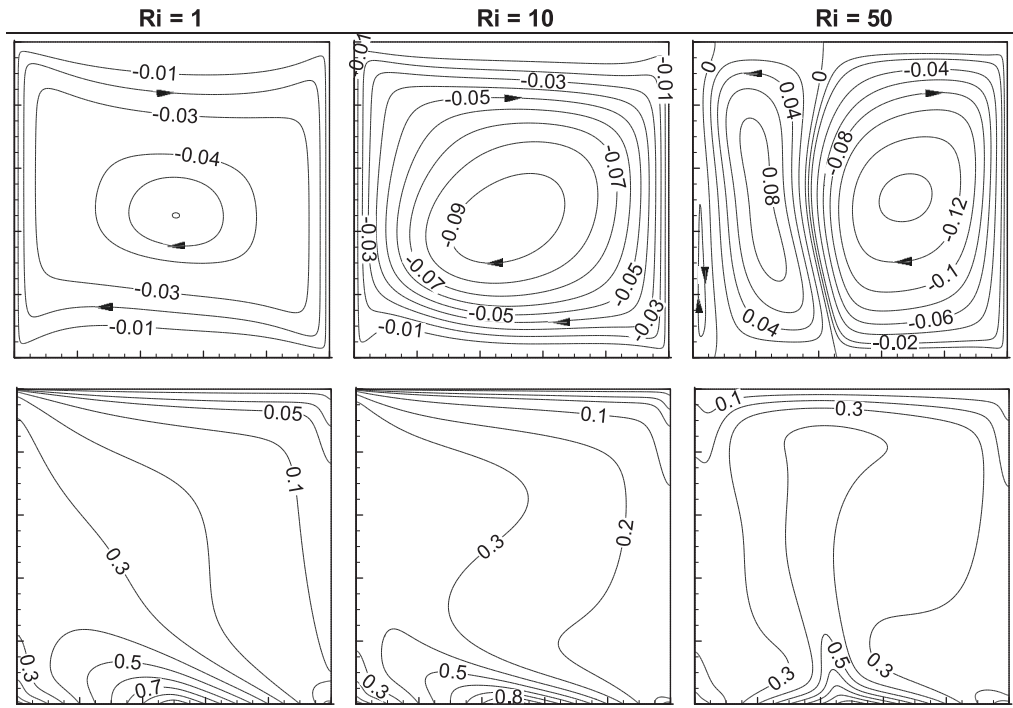


Fig.2. Effect of varying Richardson number (Ri) on flow fields (streamlines in first row) and thermal fields (isotherms in second row) for $Re = 200$, $Ha = 30$ and $\gamma = 0$.

As Ri represents the comparative strength of buoyancy force over the viscous force, so the effect of wall motion is more prominent for $Ri = 1$. As the strength of natural convection increases by adjusting higher value of Ri , the buoyancy force dominantly influences the flow structure. The vortex is clockwise due to the kinetic effect of the left and right moving walls. The presence of viscous force for the wall motion justifies the presence of a single vortex for $Ri = 1$. With increasing buoyancy force through Ri (as Re kept fixed at 200), the effect of natural convection becomes more significant as is evident by the formation of another vortex in anticlockwise direction for $Ri = 50$. The vortex at the left wall is purely due to the viscous effect of the moving left wall and no slip condition. Another important

thing can be noted from the figure is the strength of the vortex presented by the maximum value of the streamlines. For $Ri = 50$, the maximum value is almost thrice of that of $Ri = 1$ and twice of that of $Ri = 10$.

The static temperature distribution is presented by the isotherms. The hot fluid is mostly present in the bottom region of the cavity. The isotherm values of '0' and '1' respectively represent the coldest and hottest states of fluid in the cavity. The top wall of the cavity is cold ('0'). However, the bottom wall of the cavity is subjected to triangular heating from '1' (at midpoint) to '0' (at either sides). As such different values of isotherm contours are intersecting with the bottom wall and due to circulation the hotter fluid zone tends to shift towards left for lower

Ri values. It is observed that with increasing Ri, the isotherm values nearer to '1' are squeezed in the middle which is a direct result of the dominating nature of natural convection.

3.2 Effect of Reynolds number (Re)

Through streamlines and isotherms at different Re, and fixed Ri = 10 and Ha = 30, Fig. 3 demonstrates Re-effects on the heat transfer process in the cavity. The vortex pattern is mainly governed by the moving walls causing shear action on the nearby fluid layers. As Re increases vortex strength increases. The isotherm pattern is dependent on the streamline pattern (that is the presence of the vortex inside the cavity). At

lower Re value (Re = 10), isotherm pattern is almost symmetric about the mid-vertical plane. Here, the heat is mainly transported by the mode of thermal conduction. With fixed Ri = 10, as Re increases, both the strength of forced convection as well as natural convection increases. Thus, the circulation strength increases with Re; the isotherm patterns become more asymmetric and instead of getting a peak at the mid-plane, it shifts towards the left (about the mid-bottom of the cavity). It suggests that for higher Re values more amount of hot fluid reaches to the left corner region of the cavity; and thermal convection mode plays dominating role over the thermal conduction (since Gr is significantly high at higher Re when Ri is fixed at 10).

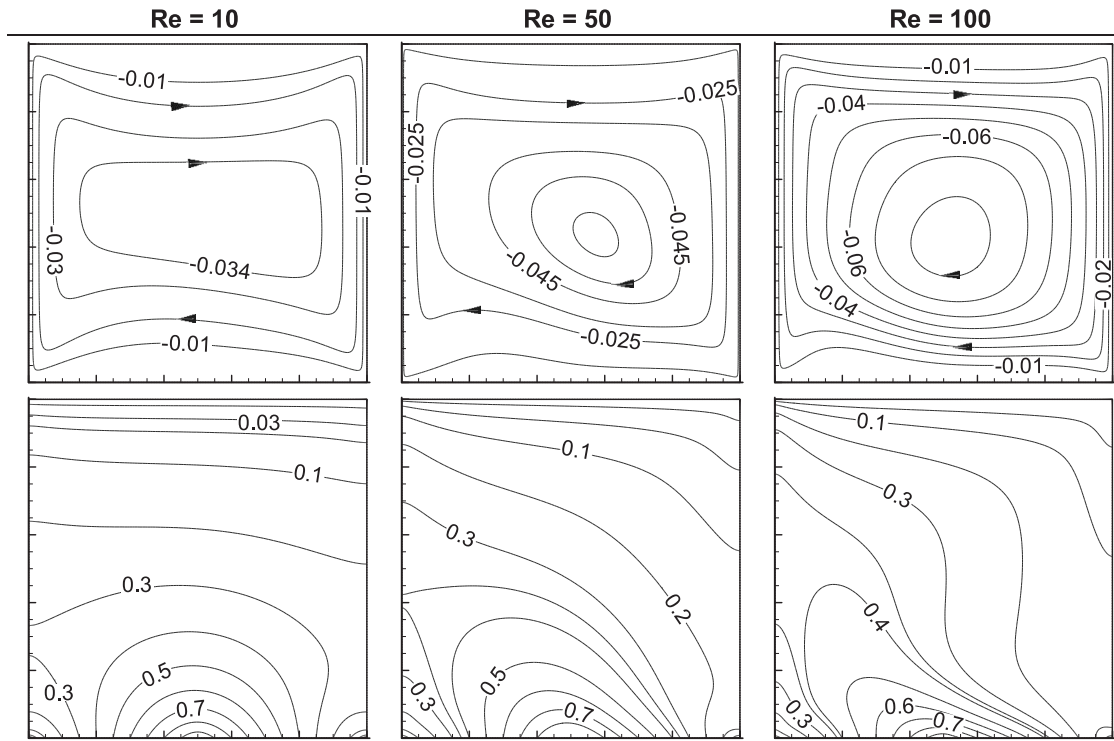


Fig.3. Effect of varying Reynolds number (Re) on flow fields (streamlines–first row) and thermal fields (isotherms–second row) for fixed Ri = 10, Ha = 30 and $\gamma = 0$.

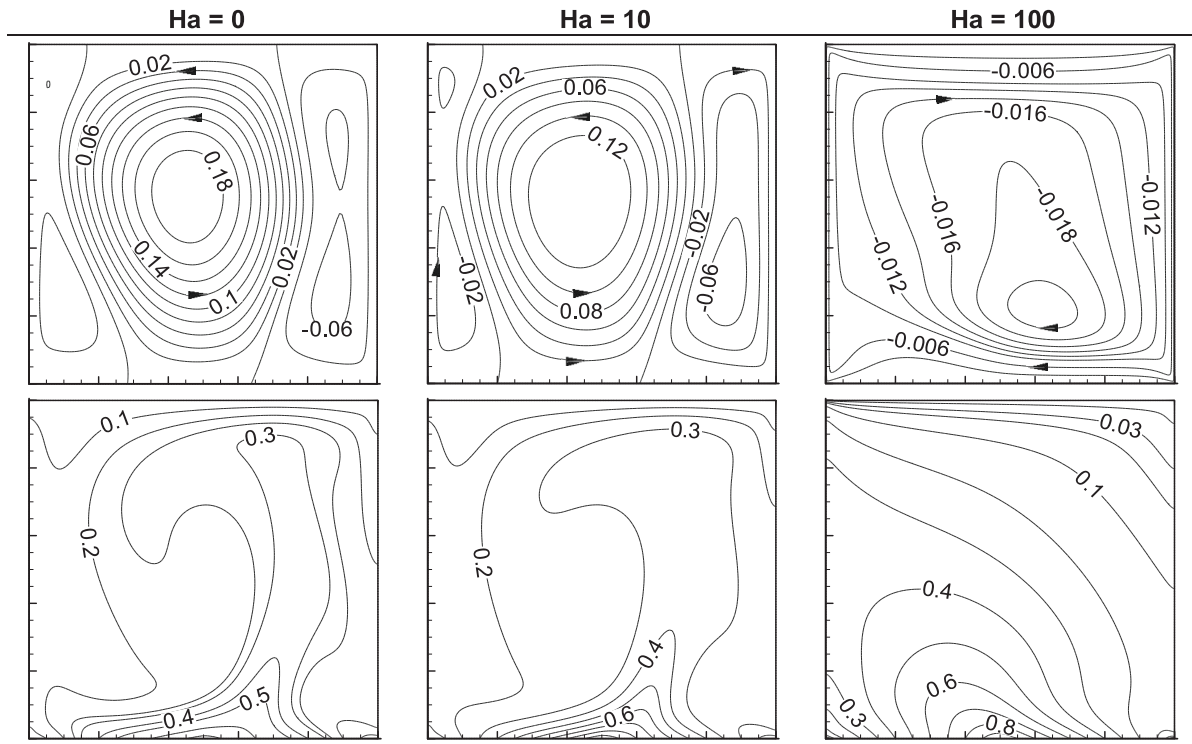


Fig. 4. Effect of Hartman number on flow fields (streamlines–first row) and thermal fields (isotherms–second row) for $Re = 200$, $Ri = 10$ and $\gamma = 0$.

3.3 Effect of Hartman number (Ha)

The magnetic force in the form of uniform magnetic field influences the structures of flow pattern and temperature distribution, which is captured using Hartman number Ha . Ha value is used to regulate the magnitude of intensity of magnetic field. Ha -effects are demonstrated in Fig. 4 using streamlines and isotherms at $Re = 200$, $Ri = 10$ and $\gamma = 0$. It is clear from the streamline plot that the strength of the counter-clockwise (CCW) central vortices at $Ha = 0$ and 10 decreases. While the size of vortices along the sidewalls rotating in clockwise (CW) direction increases with magnetic strength, there is only one CW vortex in the cavity at $Ha = 100$. This shows that with increase in magnetic

strength, forced convection dominates over natural convection. From isotherms plot, it can be observed that with increase in Ha value, rightward peaks of isotherms shift to leftward peaks. This is due to counteraction or negative impact of magnetic force, the advection in the cavity reduces, which causes decreased circulation strength.

3.4 Effect of magnetic field angle (γ°)

The change in inclination strongly affects the distribution and strength of the vortices as depicted in Fig. 5. For inclination of $\gamma = 30^\circ$, there are total three vortices (two CW and one CCW). The CW vortices on the left and right wall are mainly formed by wall-induced shear. The CCW vortex in the middle is due to

natural convection. At $\gamma = 90^\circ$ the dominance of natural convective flow is more. At the right wall, the wall motion is actually helping the natural convection induced vortex, so its strength increases. However, at the left wall they (wall induced shear flow and buoyant flow) are opposing each other, so a CW vortex on the left wall is formed. For $\gamma = 150^\circ$, forced convection dominates over natural convection. Natural convection induced CCW vortex diminishes and the CW vortices on the left and right wall get merged together to form a single stronger vortex over the entire cavity.

case ($\gamma = 30^\circ$), due to the CW vortex at the right wall, the hot fluid has little set over on the right side from the mid portion of the bottom wall. In the second case ($\gamma = 90^\circ$), due to natural convection dominance, the distribution of isotherm is almost symmetric about the mid vertical plane and the formation of plume can be observed. In the third case ($\gamma = 150^\circ$), due to the single CW vortex, more amount of hot fluid can be found on the left portion of the bottom wall. The reason behind these patterns of isotherms and streamlines can be realized from the magnetic force term in the governing equations. As the magnetic field inclines, the sharing of this force in the horizontal and vertical directions changes. It results in change in contour patterns.

The isotherm patterns are strongly dependent on circulation in the cavity. For the first

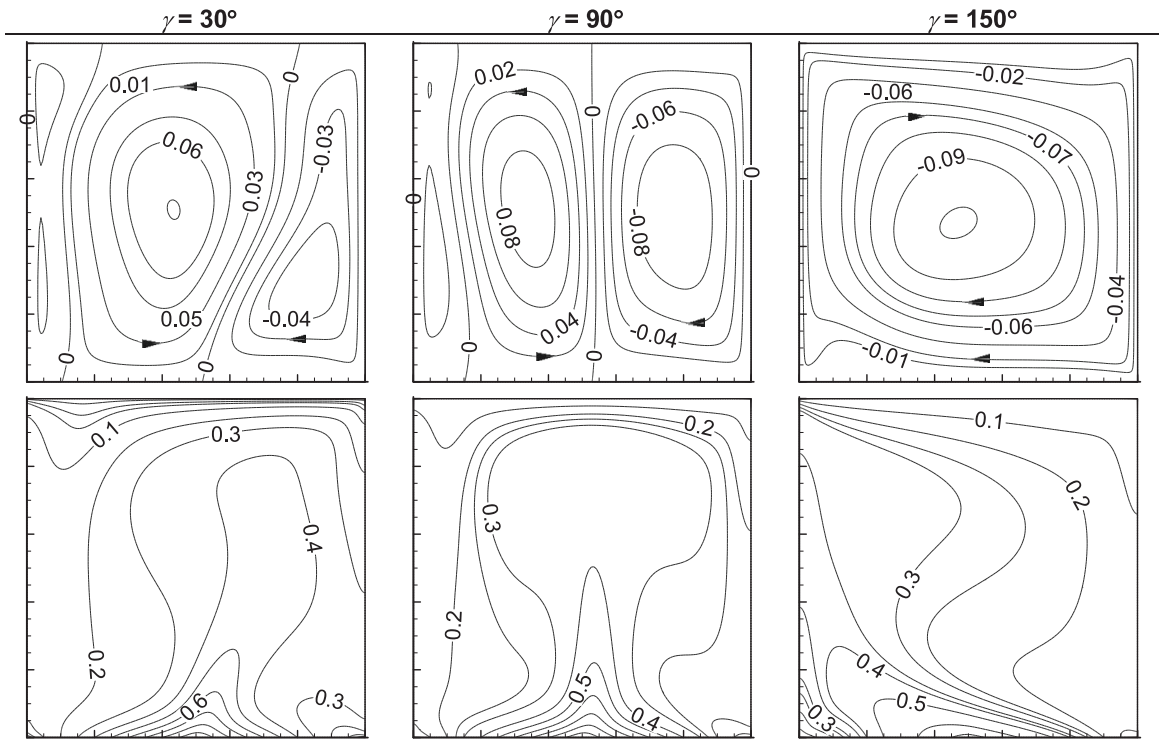


Fig.5. Effect of γ variation on flow fields (streamlines—first row) and thermal fields (isotherms—second row) for $Ha = 30$, $Re = 200$, $Ri = 10$.

3.5 Heat transfer analysis (Nu)

Fig.6 shows heat transfer characteristics for the present investigation. Fig.6a showing Nu variation against Ri indicates that heat transfer enhances almost linearly with the increment of Ri. For fixed Re (= 200) and Ha (= 30), it is expected as Ri directly increases the value of Grashof number Gr and thereby the strength of the natural convection. Fig.6b depicts that with increasing Re, heat transfer increases due to increasing thermal convection from the shear-induced flow. Furthermore, from Fig.6c, it is very clear that due to damping effect of magnetic force, the average Nu value decreases with increasing Ha. An interesting trend of the variation of heat transfer with the change in inclination of the magnetic field is observed in Fig.6d. The inclination angles around $\gamma = 90^\circ$ indicate maximum heat transfer.

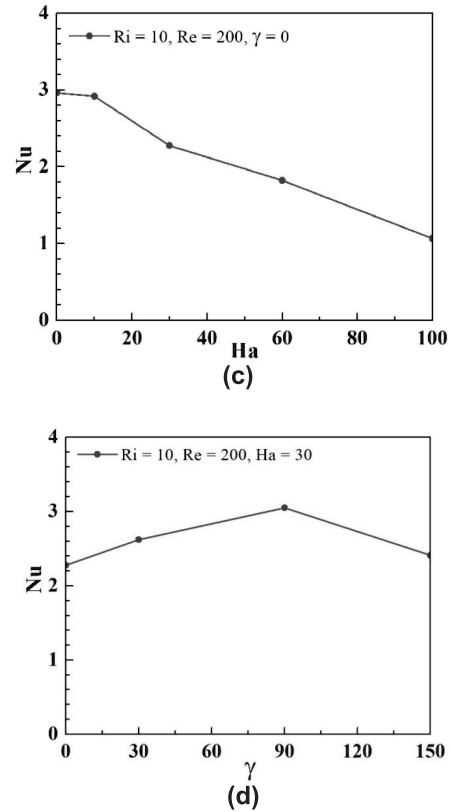
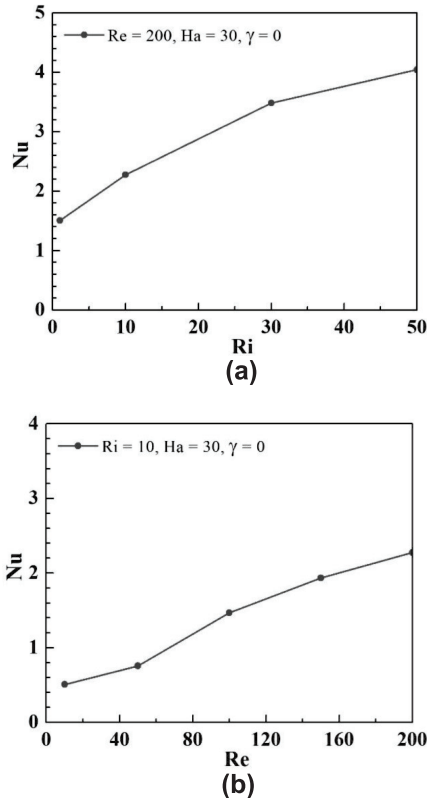


Fig. 6. Effect of parametric variation on average Nusselt number (Nu).

4. CONCLUSIONS

The study presents buoyant flow in the cavity heated linearly from the both ends of the bottom wall applying magnetic fields. The involved parameters, Re, Ri, Ha and inclination angle of magnetic field, are analyzed systematically using isotherms and streamlines along with Nusselt number. The major observations are concluded below:

- Heat transfer in terms of Nu increases with decreasing rate of increasing Ri.
- Higher Reynolds number has more impact on the heat transport in the cavity.

- From the high Nu as Ha increases, heat transfer reduces at faster rate (due to damping effect of magnetic force) affecting the flow structure severely.
- The inclination of magnetic field also markedly affects fluid flow in the cavity and thereby influences heat transfer process.

Above-mentioned observations are important for controlling thermal devices under similar configuration. The present work contributes in the area of multi-physical thermal systems involving buoyancy, magnetic force and wall-induced shear force. It would enrich the fundamental knowledge in this area and provide useful background information for design and operation of similar systems.

Acknowledgement: The present paper is based on the article presented in the National Conference on Trends and Advances in Mechanical Engineering (TAME-2019) held at Kalyani Govt. Engineering College, Kalyani on February 15-16 2019 and jointly organized by The Association of Engineers, India, Kalyani Govt. Engineering College, Kalyani and Global Institute of Management and Technology, Krishnagar as a part of the Centenary Celebration of the Association of Engineers, India.

REFERENCES

- [1] Khanafer, K.M., Al-Amiri, A.M. and Pop I, Numerical Simulation of Unsteady Mixed Convection in a Driven Cavity Using an Externally Excited Sliding Lid, *Eur J Mech B/Fluids*, Vol.26, pp.669–87, 2007.
- [2] Rahman, M.D.M., Alim M.A., Saha, S. and Chowdhury, M.K., A Numerical Study of Mixed Convection in a Square Cavity with a Heat Conducting Square Cylinder at Different Locations, *J Mech Eng. Instit Eng Bangl ME*, Vol.39, pp.78–85, 2008.
- [3] Moshizi, S.A. and Malvandi, A., Different Modes of Nanoparticle Migration at Mixed Convection of Al_2O_3 –Water Nanofluid Inside a Vertical Micro Annulus in the Presence of Heat Generation/Absorption, *J Therm Anal Calorim*, Vol.126, pp.1947–62, 2016.
- [4] Garoosi, F., Rohani, B. and Rashidi M.M., Two Phase Simulation of Natural Convection and Mixed Convection of the Nanofluid in a Square Cavity with Internal and External Heating, *Powder Technol*, Vol.75, pp.304–21, 2015.
- [5] Sivaraj, C. and Sheremet, M.A., MHD Natural Convection and Entropy Generation of Ferrofluids in a Cavity with a Non-Uniformly Heated Horizontal Plate, *Int. J Mech Sciences*, Vol.149, pp.326–337, 2018.
- [6] Akinsete, V.A. and Coleman, T., Heat Transfer by Steady Laminar Free Convection in Triangular Enclosures, *Int. J. Heat Mass Transf*, Vol.25, pp.991–998, 1982.
- [7] House, J.M., Beckermann, C. and Smith, T.F., Effect of a Centered Conducting Body on Natural Convection Heat Transfer in an Enclosure, *Numer. Heat Transfer A*, Vol.18, pp.213–225, 1990.
- [8] Hakeem, A.K.A., Saravanan, S. and Kandaswamy, P., Buoyancy

- Convection in a Square Cavity with Mutually Orthogonal Heat Generating Baffles, *Int. J. Heat Fluid Flow*, Vol.29, pp.1164–1173, 2008.
- [9] Saravanan, S. and Sivaraj, C., Combined thermal radiation and natural convection in a cavity containing a discrete heater: Effects of nature of heating and heater aspect ratio, *Int. J. of Heat Fluid Flow*, Vol.66, pp.70–82, 2017.
- [10] Karatas, H. and Derbentli, T., Natural Convection in Rectangular Cavities with One Active Vertical Wall, *Int. J. Heat Mass Transf*, Vol.105, pp.305–315, 2017.
- [11] Oztop, H.F., Abu-Nada, E., Varol, Y. and Chamkha, A., Natural Convection in Wavy Enclosures with Volumetric Heat Sources, *Int. J. Therm. Sci.* Vol.50, No.4, pp.502–514, 2011.
- [12] Sathiyamoorthy, M. and Chamkha, A.J., Natural Convection Flow under Magnetic Field in a Square Cavity for Uniformly (Or) Linearly Heated Adjacent Walls, *Int. J. Numer. Methods Heat Fluid Flow*, Vol.22, No.5, pp.677–698, 2012.
- [13] Oreper, G.M. and Szekely, J., The Effect of an Externally Imposed Magnetic Field on Buoyancy Driven Flow in a Rectangular Cavity, *J. Crystal Growth*, Vol.64, pp.505–515, 1983.
- [14] Ozoe, H. and Maruo, M., Magnetic and Gravitational Natural Convection of Melted Silicon-Two Dimensional Numerical Computations for the Rate of Heat Transfer, *JSME*, Vol.30, pp.774–784, 1987.
- [15] Bondareva, N.S. and Sheremet, M.A., Effect of Inclined Magnetic Field on Natural Convection Melting in a Square Cavity with a Local Heat Source, *ýJ. Magn. Mater*, Vol.419, pp.476–484, 2016.
- [16] Biskamp D., *Magneto hydrodynamic Turbulence*, Cambridge University Press, Cambridge, 2003.
- [17] Kabeel, A.E., El-Said, E.M.S. and Dafea, S.A., A Review of Magnetic Field Effects on Flow and Heat Transfer in Liquids: Present Status and Future Potential for Studies and Applications, *Renew. Sus. Energy Reviews*, Vol. 45, pp.830–837, 2015.
- [18] Biswas, N., Mahapatra, P.S. and Manna N.K., Enhanced Thermal Energy Transport Using Adiabatic Block Inside Lid Driven Cavity, *Int. J. Heat Mass Transfer*, Vol.100, pp.407–427, 2016.
- [19] Biswas, N. and Manna, N.K., Transport Phenomena in a Sidewall-Moving Bottom-Heated Cavity Using Heatline, *Sadhana*, Vol.42(2), pp.193–211, 2017.
- [20] Biswas, N., Mahapatra, P.S. and Manna N.K., Enhanced Convective Heat Transfer in Lid-Driven Porous Cavity With Aspiration, *Int. J. Heat Mass Transfer*, Vol.114, pp.430–452, 2017;.